Journal of Energy Storage 60 (2023) 106586

Contents lists available at ScienceDirect

Journal of Energy Storage

journal homepage: www.elsevier.com/locate/est

Research Papers

The impact of random porosity distribution on the composite metal foam-phase change heat transfer for thermal energy storage

Mehdi Fteiti [a,*], Mehdi Ghalambaz [b,*], Mikhail Sheremet [c], Mohammad Ghalambaz [c]

[a] Physics Department, Faculty of Applied Science, Umm Al-Qura University, Makkah 24381, Saudi Arabia
[b] Institute of Research and Development, Duy Tan University, Da Nang 550000, Viet Nam
[c] Laboratory on Convective Heat and Mass Transfer, Tomsk State University, 634045 Tomsk, Russia

ARTICLE INFO

Keywords:
Random porous media
Latent heat storage
Porosity distribution
Phase change material

ABSTRACT

The goal of this work is to investigate the phase change material (PCM) embedded with a high thermal conductive solid structure (metal foam). In order to boost the effective heat conductivity and therefore quicken the storage process, metal foam is incorporated. The resultant storage medium is handled as a porous material. Most of earlier investigations of a similar type assumed that the medium's porosity in the porous zone is uniform. However, a random porosity is more accurate and realistic. Various sets of random structures were created using a pseudo-random generator. The mathematical formulation utilizes the Darcy-Brinkman model and volume-averaging method. The governing equations are numerically solved using the control-volume-based finite element approach. Various samples with high random porosity distributions were simulated and compared to the case of uniform porosity. The results were reported in the form of isotherms, liquid fractions, and streamlines. The outcomes revealed that a random porous medium could provide a lower rate of PCM melting (up to 10 %) for a similar average porosity compared to a uniform porous medium.

1. Introduction

A technique known as thermal energy storage (TES) uses heat or cold to store thermal energy that may subsequently be used for power production, heating and cooling systems, and other purposes. When compared to sensible heat storage, latent heat storage employing PCM (phase change material) exhibits a higher storage capability. However, there are some major drawbacks to the use of PCMs, such as low volumetric latent heat storage capacity and low thermal conductivity. Various methods have been suggested to enhance thermal storage performance. One effective method relies on enhancing phase transient heat transfer by embedding the PCM in open metallic foams [1]. Designing energy storage systems requires a fundamental understanding of flow and heat transmission in porous media as well as the impact of shape and pore distribution. The topic of phase change in a porous medium is vast and has been extensively investigated [2].

There are two approaches for the modeling of porosity distribution in porous media. Most of the previous studies have modelled the porous media with uniform porosity. Another more accurate approach considers a non-uniform or random porosity distribution. It has been shown that the randomness of porous structures has significant effects on permeability and heat transfer characteristics [3]. Recently many approaches, such as using nanofluids [4], boiling heat transfer [5], and corrugated tubes [6], have been employed to promote the heat transfer rate. The heating uniformity [7,8], internal heat generation [9], and drying [5] have been other important issues in recent heat transfer studies for batteries and electronic applications.

Some studies utilized metal foams with engineered structures to enhance the latent heat thermal energy storage. For example, the solid-liquid phase change heat transfer of PCMs embedded in variable porosity copper foam was numerically investigated in [10]. They considered a uniform porosity in the horizontal direction and a linear vertical gradient in the vertical direction. Alomar [11] investigated the effects of variable porosity interior porous media close to the wall border and the related phase transition processes. Their findings demonstrated that at large values of porosity and pore diameter, the impacts of variable porosity are more prominent. Also, the onset and completion of the phase change process are severely affected by the addition of the influence of variable porosity. Zhuang et al. [12] investigated the effects of gradient porous metal foam on the heat storage capabilities of latent

* Corresponding authors.
E-mail addresses: mafteiti@uqu.edu.sa (M. Fteiti), ghalambaz.mehdi@gmail.com (M. Ghalambaz), sheremet@math.tsu.ru (M. Sheremet), m.ghalambaz@gmail.com (M. Ghalambaz).

https://doi.org/10.1016/j.est.2022.106586
Received 14 September 2022; Received in revised form 10 December 2022; Accepted 29 December 2022
Available online 13 January 2023

heat thermal energy storage and the 3D melting heat transfer. According to their findings, the gradient porosity's effect on the competitive relationship between conduction and convection impacts heat transfer and energy storage. Zhang and He [13] numerically investigated the phase transition in an open-celled metal foam considering porosity gradient. To improve the melting process, they evaluated two different types of metal foam with varying porosities. Their findings showed that by improving the heat-transfer mechanism, the metal foam with a porosity gradient enhanced the rate of heat storage.

Considering the porous structure effects, Marri al. [14] experimentally and numerically investigated the effect of metal foams' porosity and pore density gradients on the thermal efficiency of a heat sink made of a composite phase-change material. Their results conveyed that the PCM melt percentage dramatically alters convection velocity in cells, which impacts PCM melting dynamics. Similar research was done, but with a horizontal porosity gradient, by Ghalambaz et al. [15]. It should be noted that whether natural or artificial, porous materials all display some degree of randomness. Computational and experimental research on the PCM melting in metal foams with random pore distributions was undertaken by Zilong et al. [16], who were inspired by the fractal theory.

There are few papers in the literature review discussing the phase transition in a porous medium of random porosity. Nevertheless, numerous investigations have been done on fluid flow, heat transfer, and mass transfer in random porous medium without phase change Fu et al. [17]. Very recently, Fteiti [18] examined the melting heat transfer of a PCM embedded in a random porous medium. The author simulated the melting process for three random porous distributions with an average porosity of about 0.7. The results showed that a random porosity (non-uniform porosity) could delay the melting heat transfer.

The metal foams are not precisely uniform, and the medium's porosity distribution could vary within the domain, notably even when the average porosity could remain constant. The literature review shows that metal foams with a high porosity of 0.9 or higher [19–21] are produced and used for thermal energy storage enhancement. However, the impact of the random porosity of the foam on the thermal behaviour of the composite metal foam-PCM is not well understood yet for a foam with high porosity. Thus, the present study aims to address the impact of random porosity distribution on the melting heat transfer of high-porosity composite metal foam-PCMs for the first time.

2. Mathematical model

The computational domain consists of a square enclosure saturated with a PCM filled with porous metal foam (Fig. 1). Initially, the domain is occupied with the Newtonian liquid phase under the laminar flow regime. The phase change is induced by the natural convection mechanism due to the asymmetric thermal boundary conditions. Adiabatic thermal boundary conditions are set for the cavity walls except for the left wall, which is kept at the constant temperature T_H higher than the PCM melting temperature T_m. The Boussinesq rule is applied to connect the density and temperature gradients.

It should be noted that it is assumed that the PCM and the matrix structure are in thermal equilibrium through the domain. Moreover, the volume change due to the phase change is considered negligible.

In a typical mathematical model based on a representative elementary volume (REV), the detailed structure of the porous medium cannot be seen in the mathematical model. Instead, the effect of porous structure would enter porosity, permeability, thermal conductivity, etc. Thus, a local change of porous structure would result in the local adaptation of REV, which was seen in the governing equations. Thus, in the context of the present study, the random porous structure is reflected in the random porosity distribution at a REV scale. As a result, the present model considers a mathematical model with a random porosity distribution. Pseudo-random is a terminology in which codes and software generate the random distribution within criteria.

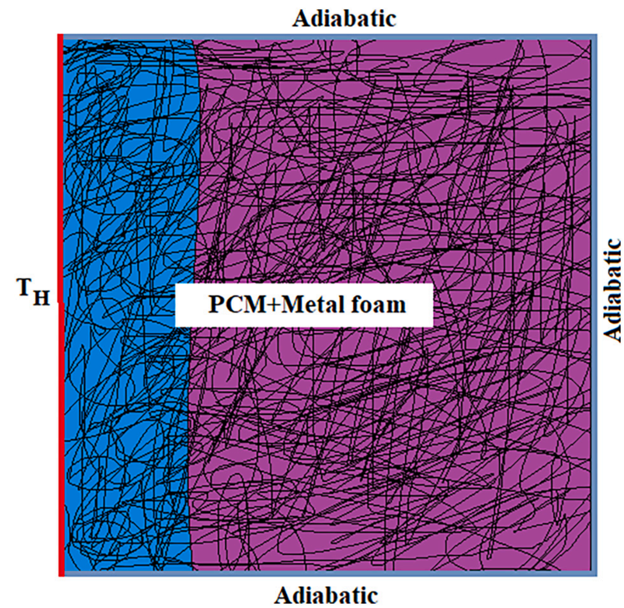

Fig. 1. Schema of the physical domain.

The transport governing equations in the porous media are modelled using the Darcy-Brinkman model and the volume averaging method [22]. Moreover, the phase change between the solid-liquid is modelled with the enthalpy-porosity technique [23]. Therefore, based on the above assumptions, the governing equations can be described as [19,20,24]:

Continuity equation

$$\frac{\partial u}{\partial x}+\frac{\partial v}{\partial y}=0. \tag{1}$$

Momentum equations in x and y directions

$$\frac{1}{\varepsilon}\frac{\partial u}{\partial t}+\frac{1}{\varepsilon^2}\left(u\frac{\partial u}{\partial x}+v\frac{\partial u}{\partial y}\right) = -\frac{1}{\rho}\frac{\partial p}{\partial x}+\frac{\nu}{\varepsilon}\left(\frac{\partial^2 u}{\partial x^2}+\frac{\partial^2 u}{\partial y^2}\right)-\frac{\nu}{K}u+S\cdot u \tag{2a}$$

$$\frac{1}{\varepsilon}\frac{\partial v}{\partial t}+\frac{1}{\varepsilon^2}\left(u\frac{\partial v}{\partial x}+v\frac{\partial v}{\partial y}\right) = -\frac{1}{\rho}\frac{\partial p}{\partial y}+\frac{\nu}{\varepsilon}\left(\frac{\partial^2 v}{\partial x^2}+\frac{\partial^2 v}{\partial y^2}\right)-\frac{\nu}{K}v+\rho g\beta_T(T-T_m)+S\cdot v \tag{2b}$$

Energy equation with phase change

$$(\rho C_p)^*\frac{\partial T}{\partial t}+(\rho C_p)_l\left(u\frac{\partial T}{\partial x}+v\frac{\partial T}{\partial y}\right)=\frac{\partial}{\partial x}\left(\lambda_{eff}\frac{\partial T}{\partial x}\right)+\frac{\partial}{\partial y}\left(\lambda_{eff}\frac{\partial T}{\partial y}\right)-L_H\frac{\partial f_l}{\partial t} \tag{3}$$

where K is the permeability, ε is the random porosity, λ_{eff} is the PCM/metal foam mixture's effective thermal conductivity, β_T is the liquid PCM thermal expansion, and f_l is the melted PCM local liquid fraction. Porosity is used to calculate effective thermal conductivity and effective heat capacity.

$$(\rho C_p)^* = \varepsilon\left[f_l(\rho C_p)_{pcm_l}+(1-f_l)(\rho C_p)_{pcm_s}\right]+(1-\varepsilon)(\rho C_p)_{foam} \tag{4}$$

$$\lambda_{eff}=\varepsilon\left[f_l\lambda_{pcm_l}+(1-f_l)\lambda_{pcm_s}\right]+(1-\varepsilon)\lambda_{foam} \tag{5}$$

Based on Carman-Kozney's equation [2,20], a sink-term for the liquid fraction inside the pores is included in Eqs. (2a) and (2b):

$$S=10^9\frac{(1-f_l)^2}{(f_l^3+0.001)} \tag{6}$$

The sink term manages the solidified zone's velocity dampening. These non-dimensional variables are formulated as:

$$X = \frac{x}{H},\quad Y = \frac{y}{H},\quad F_o = \frac{\alpha t}{H^2},\quad U = \frac{uH}{\alpha}, \tag{7a}$$

$$V = \frac{vH}{\alpha},\quad P = \frac{pH^2}{\alpha^2 \rho},\quad \text{and}\quad \theta = \frac{T - T_m}{T_H - T_m}. \tag{7b}$$

Here, α stands for the thermal diffusivity of the PCM, and H indicates the height of the cavity. The aforementioned system of equations is represented in the dimensionless form:

$$\frac{\partial U}{\partial X} + \frac{\partial V}{\partial Y} = 0, \tag{8}$$

$$\frac{1}{\varepsilon}\frac{\partial U}{\partial F_o} + \frac{1}{\varepsilon^2}\left(U\frac{\partial U}{\partial X} + V\frac{\partial U}{\partial Y}\right) = -\frac{\partial P}{\partial X} + \frac{\sigma_1}{\sigma_2}\frac{Pr}{\varepsilon}\left(\frac{\partial^2 U}{\partial X^2} + \frac{\partial^2 U}{\partial Y^2}\right) - \frac{\sigma_1}{\sigma_2}\frac{Pr}{Da}U + S.U \tag{9a}$$

$$\frac{1}{\varepsilon}\frac{\partial V}{\partial F_o} + \frac{1}{\varepsilon^2}\left(U\frac{\partial V}{\partial X} + V\frac{\partial V}{\partial Y}\right) = -\frac{\partial P}{\partial Y} + \frac{\sigma_1}{\sigma_2}\frac{Pr}{\varepsilon}\left(\frac{\partial^2 V}{\partial X^2} + \frac{\partial^2 V}{\partial Y^2}\right) - \frac{\sigma_1}{\sigma_2}\frac{Pr}{Da}V + Ra.Pr.\theta + S.V \tag{9b}$$

$$\sigma_1\frac{\partial \theta}{\partial F_o} + U\frac{\partial \theta}{\partial X} + V\frac{\partial \theta}{\partial Y} = \frac{\partial}{\partial X}\left(\sigma_2\frac{\partial \theta}{\partial X}\right) + \frac{\partial}{\partial Y}\left(\sigma_2\frac{\partial \theta}{\partial Y}\right) - \frac{1}{Ste}\frac{\partial f_l}{\partial F_o}, \tag{10}$$

where:

$$\sigma_1 = \varepsilon + (1-\varepsilon)\left(\rho C_p\right)_{foam} \Big/ \left(\rho C_p\right)_{pcm} \tag{11a}$$

and

$$\sigma_2 = \varepsilon\left[f_l + (1-f_l)\lambda_{pcm_s}/\lambda_{pcm_l}\right] + (1-\varepsilon)\left(\lambda_{foam}/\lambda_{pcm_l}\right) \tag{11b}$$

The governing Eqs. (8) through (11b) take on a set of dimensionless forms, resulting in a collection of dimensionless regulating parameters: the Stefan number $Ste = C_p \Delta T / L_H$, the Prandtl number $Pr = \nu/\alpha$, the Rayleigh number $Ra = g\beta L^3 \Delta T / \alpha\nu$, and the Darcy number $Da = K/H^2$. Here L_H, is the fusion latent heat.

The melting volume fraction is the result of the integration of f_l over the domain of the solution as:

$$MF = \frac{\int \varepsilon f_l dA}{\int dA} \tag{12}$$

where dA is the surface element of the enclosure, and porosity ε is a function of the material space (X and Y).

3. Numerical methodology, mesh study and validation

The discretization of the governing equations is handled using the CVFE model proposed by [25]. Then the TDMA solver is invoked to solve these discretized equations using the SIMPLER algorithm.

The computational domain is discretized using a staggered structured grid. A grid sensitivity analysis was performed for three different grid sizes 81 × 81, 101 × 101 and 121 × 121. The melting front position is plotted in Fig. 2 when τ = 0.1 As seen, the meshes are identical at the bottom of the enclosure. However, they are slightly different at the top region. The reason could be the natural convection effects, which are more pronounced at the top region. The difference between the melting fronts decreases with the increase in mesh size. Thus, it is evident that a mesh size of 101 × 101 can provide accurate results for visual presentation. Thus, a mesh of 101 × 101 nodes was selected as the optimum grid size, ensuring the results' independence versus the grid's resolution.

In order to evaluate the validation of the numerical approach, the case of free convective flow in a porous square cavity is simulated. The computed average Nusselt number at four different conditions of Darcy and Rayleigh numbers are compared with the results of [26]. As shown (Table 1), the maximum deviation of the current simulation results and those of Lauriat et al. are less than 1 %, which confirms the validity of the simulations.

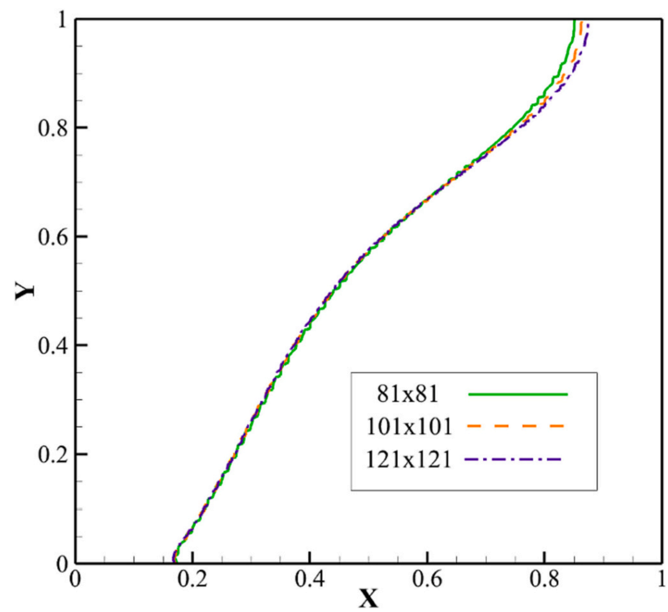

Fig. 2. Melting front at the dimensional time $\tau = 0.1$ for the grid sizes 81 × 81, 101 × 101, and 121 × 121.

Table 1
Comparison of the average Nusselt number of the current simulations with the literature at ($A = 1$ and $Pr = 0.71$).

Study	$Ra \times Da$	$Da = 10^{-5}$	$Da = 10^{-2}$
Present work	500	8.42	3.30
Lauriat et al. [26]	500	8.41	3.30
Present work	0.4260	12.45	4.26
Lauriat et al. [26]	0.4650	12.42	4.26

To validate the phase change model, a melting test of pure Gallium was performed in a rectangular cavity of height $H = 6.35$ cm and width $L = 8.89$ cm, heated from the left side to a temperature $T_H = 38$ °C and cooled at the right vertical side $T_C = 27$ °C (1 °C below the melting temperature of the pure Gallium). Results are compared with the experimental results of [27]. Several other numerical solutions [23,28–30], where the front position is plotted at times τ = 0.41 ($t = 2$ min), τ = 1.23 ($t = 6$ min), τ = 2.05 ($t = 10$ min), and τ = 3.48 ($t = 17$ min) in Fig. 3. The figure shows the current simulations agree to the trend of numerical and experimental data available in the literature.

4. Results and discussions

In this study, the effect of the porosity distributions on the location of the liquid-solid interface and the flow and temperature field patterns are examined. Moreover, the evolution of the melting process during natural convection is investigated. As mentioned earlier, the domain is filled with a random porous structure, and the porosity distribution of the media is modelled using a pseudo-random number generator code. Three samples of the generated random porous media are shown in Fig. 4 and named Run1, Run2, and Run3. Notably, these three cases with patterns are unique patterns that have almost identical mean porosity.

The local porosity denotes the average amount of the metal foam at each local coordinate. Considering a high porosity metal foam with randomly distributed pores, any cross-section of the structure results in a random 2D local porosity distribution. Hence, any cross-section leads to a new sample of 2D random distribution. Thus, the trend of the results of the 2D case could then be extended to the 3D configuration. The filled contours of the porosity distributions generated randomly are displayed

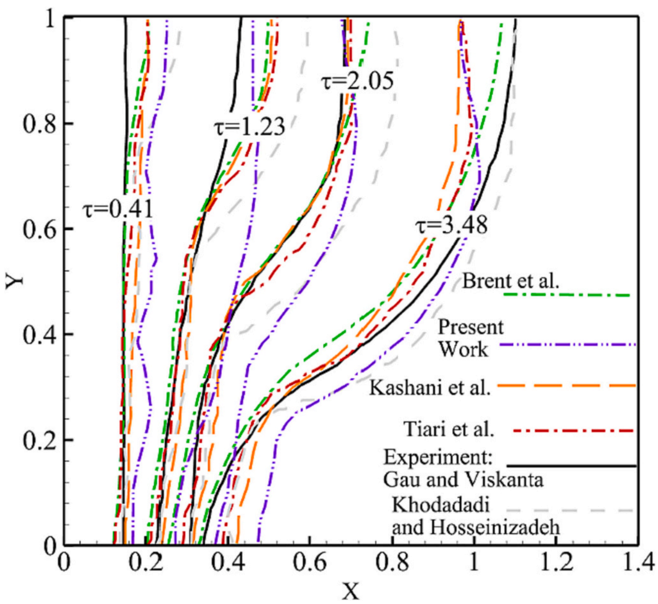

Fig. 3. Comparison of the melting interface during the phase change of pure material $Ra = 6 \times 105$ and $Pr = 0.0216$. The simulation results of the current study, the experimental results of [21], and numerical data [17,22–24].

in Fig. 4, which clearly shows the randomness of the distribution. The porosity changes by about 0.9 with a standard deviation of 0.058. It should be noted that an actual porous structure was not created in the present study. Instead, the impact of local porosity variations was entered into the mathematical model through a random porosity distribution, as depicted in Fig. 4.

The random porosity distribution can be confirmed in Fig. 5, where graphs of the porosity distribution are plotted along the horizontal axis at the mid-height of the cavity ($Y = 0.5$) for the three Runs where no relationship between the graphs could be noticed. Table 2 shows the statistical characteristics of each of the random porous distributions.

To analyze the effect of the randomness of the porosity distribution and the interaction with natural convection, the mentioned simulations are performed at dimensionless parameters of $Ra = 5.0 \times 10^6$, $Pr = 50$, $Ste = 0.1$ and $Da = 10^{-3}$. As an interesting point, the melting process in a uniform porosity porous medium with a mean porosity $\overline{\varepsilon} = 0.9$ is compared with the considered random porous media. As illustrated in Fig. 6, liquid-solid interface positions at two different non-dimensional times $\tau = 0.1$ and $\tau = 0.2$ are compared.

Since the interface advancement for the uniform porosity is superior, it can be inferred that the melting rate is reduced in the random porosity cases. It was noted that the uniform porosity case dampens the intrinsic morphological homogeneity of the porous structure, which leads to a low dispersion of heat due to its uniform thermal properties. Hence, the PCM melting is intensified by the dominance of natural convection, leading to faster interface advancement.

However, as the random porosity distribution is more realistic and better models the physics of a porous media, it is expected to have a weaker rate of natural convection due to the higher dispersion terms. Therefore, in the random cases, the interface advancement is slower, its interface shape fluctuates, and it is non-smooth. Besides, Fig. 7 compares the transient melting volume fraction of the uniform and random porosity distribution metal foams. When $\tau = 0.3$, the melting volume fraction is 0.75 and 0.84 for random and uniform porosity cases. Thus, the random porosity reduced the melting process by about 10 %, i.e., $100 \times (0.84 - 0.75) / 0.84$.

It can be seen that the uniform porosity case has a faster interface advancing over the random cases. However, all cases simultaneously reach a full melting (melt fraction = 0.9) ($\tau = 0.5$). For a case of low porosity ($\overline{\varepsilon} = 0.7$), the complete melting for a uniform case reaches much faster than a non-uniform case [18]. Moreover, using a high amount of metal foam ($\overline{\varepsilon} = 0.7$) results in a full melting time of about $\tau = 0.25$ [18]. It should be noted that using foam with porosity $\overline{\varepsilon} = 0.9$ reduces the latent heat capacity of the enclosure by 10 %. In contrast, for a case of low porosity ($\overline{\varepsilon} = 0.7$), the reduction in the latent heat capacity of the enclosure is 30 %.

A comparison of the resultant streamlines in the random and uniform porosity cases is shown in Fig. 8. It can be seen that the random cases have nearly identical streamlines. However, due to the larger extent of the melting process in the uniform porous media, the streamlines are more spread in this case. Similarly, the variations of the isothermal lines in the random and uniform porosity cases are shown in Fig. 9. This plot indicates that the fluctuation of isothermal lines in the random cases is behind the uniform case. Thus, the uniform case has covered a larger molten region. These findings agree with the MVF results discussed in Fig. 7.

5. Conclusions

The current study numerically dealt with the PCM melting in a porous medium. Two distinct types of porosity distribution were considered, i.e., uniform and random. The results showed that the random cases have nearly identical but fluctuating behaviour at the same average porosity condition. Moreover, the uniform porous media had a higher rate of PCM melting, which was distinguishable from the random cases. The random porosity could reduce the melting volume fraction up to 10 %.

Also, the PCM melting is intensified by the dominance of natural convection, leading to faster interface advancement. Since the nature of

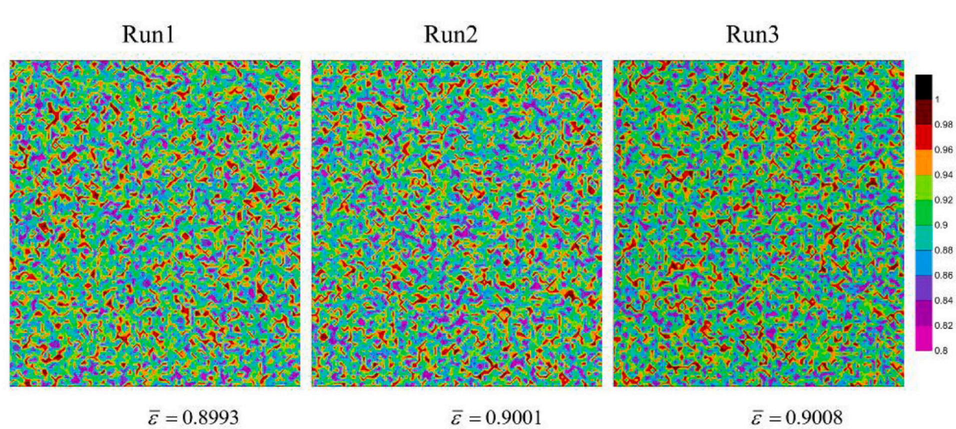

Fig. 4. Random samples of the porous structure; the row porosity data has been provided here https://doi.org/10.17632/h32cdrvk78.1.

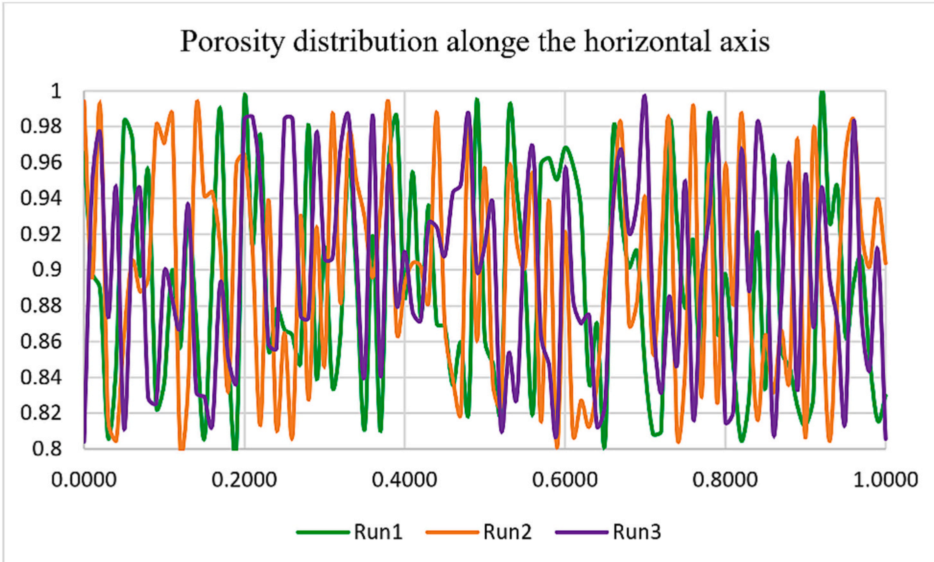

Fig. 5. Axial distribution of the porosity.

Table 2
Statistical parameters of the random samples.

Study	Run1	Run2	Run3
Mean porosity	0.8993	0.9011	0.9008
Median	0.8993	0.9013	0.9018
Standard deviation	0.0583	0.0575	0.0575
Variance	0.0034	0.0033	0.0033
Skewness	0.0094	−0.0229	−0.0253
Kurtosis	1.7830	1.8083	1.8047

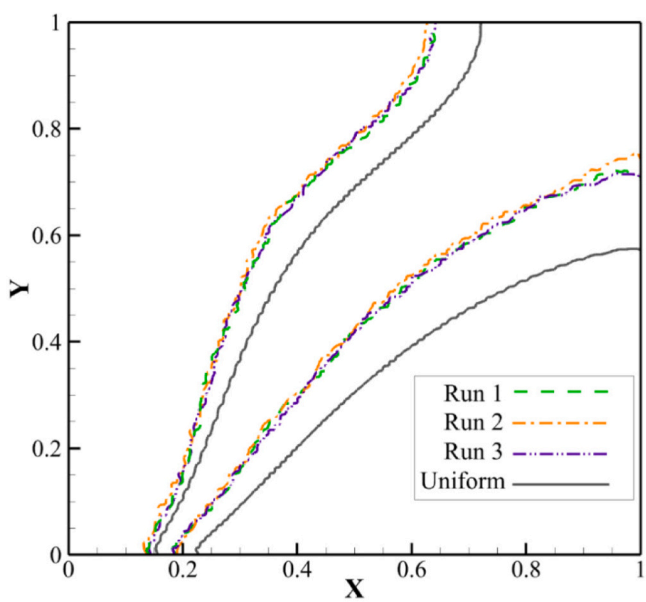

Fig. 6. Comparison of interface location of random and uniform porous media at two dimensionless times. The details of each run have been specified in Table 2.

porous media has some morphological inhomogeneities, care must be taken in selecting uniform porous media in the numerical simulations. Since the present results showed that random porosity influences the melting process notably, the authors suggest conducting some experimental studies to investigate these issues deeply.

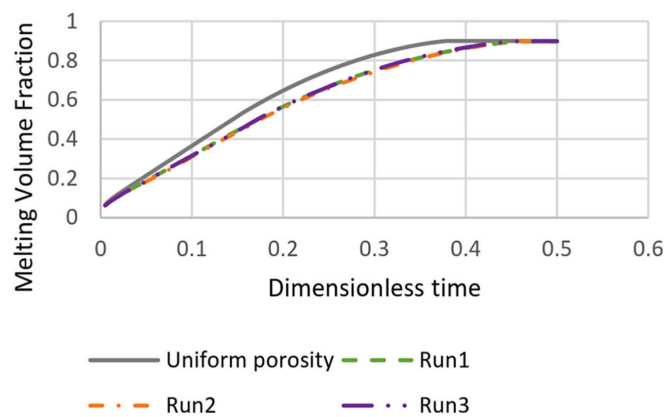

Fig. 7. Time evolution of melting fraction. Comparison between random and uniform porous media.

Here, as a pioneer study, a 2D model and distribution of random porosity were adopted. The 2D model provides a general trend of behaviour for the impact of random porosity on the melting heat transfer. The results showed that the random porosity could significantly reduce heat transfer and slow down the melting process. Moreover, it should be noted that a metal foam is generally a 3D structure, and thus, the random porosity distribution has a general 3D distribution. Therefore, the study of a 3D random porosity impact on the melting heat transfer can be the subject of future studies to provide a more detailed analysis.

CRediT authorship contribution statement

M. Fteiti: Conceptualization, Methodology, Software, Validation, Formal analysis, Data Curation. Mehdi Ghalambaz: Visualization, Original draft preparation, Investigation. Formal analysis, Data curation. M. Sheremet: Methodology, Software; Formal analysis, Data curation. Mohammad Ghalambaz: Investigation, Writing - review & editing. Supervision.

Declaration of competing interest

The authors clarify that there is no conflict of interest for report.

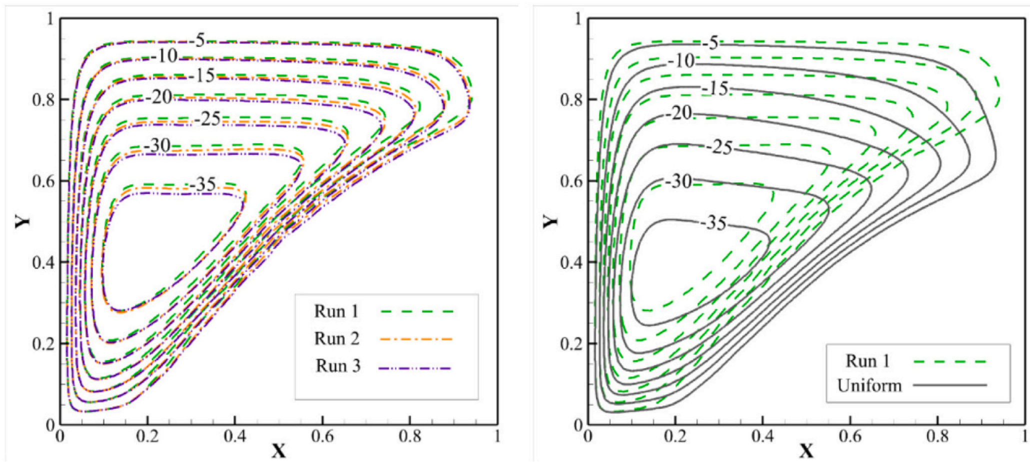

Fig. 8. Calculated streamlines for the random porous medium (left) and uniform porous medium (right).

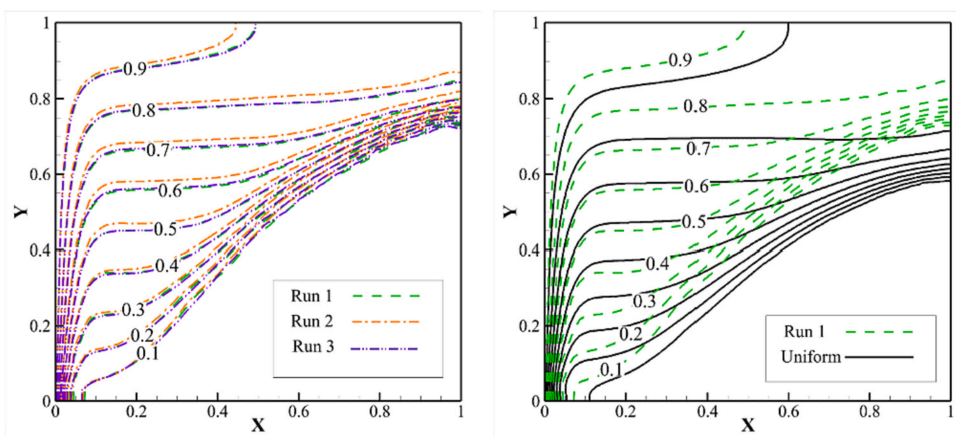

Fig. 9. Isotherms for the random porous medium (left) and uniform porous medium (right).

Data availability

Data will be made available on request.

Acknowledgements

The authors would like to thank the Deanship of Scientific Research at Umm Al-Qura University for supporting this work by Grant Code: (22UQU4310414DSR05). This research of Mohammad Ghalambaz and Mikhail Sheremet was supported by the Tomsk State University Development Programme (Priority-2030).

References

[1] J. Chen, D. Yang, J. Jiang, A. Ma, D. Song, Research progress of phase change materials (PCMs) embedded with metal foam (a review), Procedia Mater. Sci. 4 (2014) 389–394.
[2] D.A. Nield, A. Bejan, Convection in Porous Media, Springer, 2006.
[3] A. Sanjari, M. Abbaszadeh, A. Abbassi, Lattice Boltzmann simulation of free convection in an inclined open-ended cavity partially filled with fibrous porous media, J. Porous Media 21 (2018) 1265–1281.
[4] W.T. Yan, C. Li, W.B. Ye, Numerical investigation of hydrodynamic and heat transfer performances of nanofluids in a fractal microchannel heat sink, Heat Transfer Asian Res. 48 (2019) 2329–2349.
[5] W.T. Yan, W.B. Ye, C. Li, Effect of aspect ratio on saturated boiling flow in microchannels with non-uniform heat flux, Heat Transfer Asian Res. 48 (2019) 3312–3327.
[6] J. Du, Y. Hong, S. Wang, W.-B. Ye, S.-M. Huang, Experimental thermal and flow characteristics in a traverse corrugated tube fitted with regularly spaced modified wire coils, Int. J. Therm. Sci. 133 (2018) 330–340.
[7] W.-B. Ye, Thermal simulation and evaluation for non-uniformity detection of electrode, Appl. Therm. Eng. 96 (2016) 583–592.
[8] W.-B. Ye, Finite volume analysis the thermal behavior of electrode non-uniformity, Heat Mass Transf. 53 (2017) 1123–1132.
[9] W.-B. Ye, C. Li, S.-M. Huang, Y. Hong, Validation of thermal modeling of unsteady heat source generated in a rectangular lithium-ion power battery, Heat Transfer Res. 50 (2019).
[10] J. Yang, L. Yang, C. Xu, X. Du, Numerical analysis on thermal behavior of solid–liquid phase change within copper foam with varying porosity, Int. J. Heat Mass Transf. 84 (2015) 1008–1018.
[11] O.R. Alomar, Analysis of variable porosity, thermal dispersion, and local thermal non-equilibrium on two-phase flow inside porous media, Appl. Therm. Eng. 154 (2019) 263–283.
[12] Y. Zhuang, Z. Liu, W. Xu, Effects of gradient porous metal foam on the melting performance and energy storage of composite phase change materials subjected to an internal heater: a numerical study and PIV experimental validation, Int. J. Heat Mass Transf. 183 (2022), 122081.
[13] Z. Zhang, X. He, Three-dimensional numerical study on solid-liquid phase change within open-celled aluminum foam with porosity gradient, Appl. Therm. Eng. 113 (2017) 298–308.
[14] G.K. Marri, C. Balaji, Experimental and numerical investigations on the effect of porosity and PPI gradients of metal foams on the thermal performance of a composite phase change material heat sink, Int. J. Heat Mass Transf. 164 (2021), 120454.
[15] M. Ghalambaz, S. Mehryan, A. Hajjar, M.A. Fteiti, O. Younis, P.T. Sardari, W. Yaïci, Latent heat thermal storage in non-uniform metal foam filled with nano-enhanced phase change material, Sustainability 13 (2021) 2401.
[16] Z. Deng, X. Liu, C. Zhang, Y. Huang, Y. Chen, Melting behaviors of PCM in porous metal foam characterized by fractal geometry, Int. J. Heat Mass Transf. 113 (2017) 1031–1042.
[17] W.-S. Fu, W.-W. Ke, Effects of a random porosity model on double diffusive natural convection in a porous medium enclosure, Int. Commun. Heat Mass Transf. 27 (2000) 119–132.

[18] M.A. Fteiti, Latent heat storage in a random porosity metal foam filled with a phase change material, in: 13th International Exergy, Energy and Environment Symposium (IEEES-13), Makkah, Saudi Arabia, 2021.
[19] P. Talebizadehsardari, H.I. Mohammed, J.M. Mahdi, M. Gillott, G.S. Walker, D. Grant, D. Giddings, Effect of airflow channel arrangement on the discharge of a composite metal foam-phase change material heat exchanger, Int. J. Energy Res. 45 (2021) 2593–2609.
[20] P.T. Sardari, R. Babaei-Mahani, D. Giddings, S. Yasseri, M. Moghimi, H. Bahai, Energy recovery from domestic radiators using a compact composite metal foam/PCM latent heat storage, J. Clean. Prod. 257 (2020), 120504.
[21] S. Huang, J. Lu, Y. Li, Numerical study on the influence of inclination angle on the melting behaviour of metal foam-PCM latent heat storage units, Energy 239 (2022), 122489.
[22] S. Whitaker, The Method of Volume Averaging, Springer Science & Business Media, 2013.
[23] A. Brent, V.R. Voller, K. Reid, Enthalpy-porosity technique for modeling convection-diffusion phase change: application to the melting of a pure metal, Numer. Heat Transf. Part A Appl. 13 (1988) 297–318.
[24] J.M. Mahdi, H.I. Mohammed, P. Talebizadehsardari, M. Ghalambaz, H.S. Majdi, W. Yaïci, D. Giddings, Simultaneous and consecutive charging and discharging of a PCM-based domestic air heater with metal foam, Appl. Therm. Eng. 197 (2021), 117408.
[25] B. Baliga, S. Patankar, A new finite-element formulation for convection-diffusion problems, Numer. Heat Transfer 3 (1980) 393–409.
[26] G. Lauriat, V. Prasad, Natural convection in a vertical porous cavity: a numerical study for brinkman-extended darcy formulation, J. Heat Transf. 109 (1987) 688–696.
[27] C. Gau, R. Viskanta, Melting and solidification of a pure metal on a vertical wall, J. Heat Transf. 108 (1986) 174–181.
[28] J. Khodadadi, S. Hosseinizadeh, Nanoparticle-enhanced phase change materials (NEPCM) with great potential for improved thermal energy storage, Int. Commun. Heat Mass Transfer 34 (2007) 534–543.
[29] S. Kashani, A. Ranjbar, M. Abdollahzadeh, S. Sebti, Solidification of nano-enhanced phase change material (NEPCM) in a wavy cavity, Heat Mass Transf. 48 (2012) 1155–1166.
[30] S. Tiari, S. Qiu, M. Mahdavi, Numerical study of finned heat pipe-assisted thermal energy storage system with high temperature phase change material, Energy Convers. Manag. 89 (2015) 833–842.